



## Two-Color Laser-Plasma Generation of Terahertz Radiation Using a Frequency-Tunable Half Harmonic of a Femtosecond Pulse

N. V. Vvedenskii,<sup>1,2,\*</sup> A. I. Korytin,<sup>1</sup> V. A. Kostin,<sup>1,2</sup> A. A. Murzanev,<sup>1</sup> A. A. Silaev,<sup>1,2</sup> and A. N. Stepanov<sup>1</sup>

<sup>1</sup>*Institute of Applied Physics, Russian Academy of Sciences, Nizhny Novgorod 603950, Russia*

<sup>2</sup>*University of Nizhny Novgorod, Nizhny Novgorod 603950, Russia*

(Received 18 July 2013; published 7 February 2014)

We investigate for the first time, both experimentally and theoretically, low-frequency terahertz (THz) emission from the ambient air ionized by a two-color femtosecond laser pulse containing, besides the fundamental-frequency main field, a weak additional field tunable near the frequency of the half harmonic. By controlling the mutual polarization and the powers of the main and additional fields, we determine the dependences of the THz power and polarization on the parameters of the two-color pulse. We also discover the resonantlike dependence of the THz yield on the frequency detuning of the additional field. The analytical formulas obtained using the model of the free-electron residual current density give an excellent agreement with the experimental results.

DOI: [10.1103/PhysRevLett.112.055004](https://doi.org/10.1103/PhysRevLett.112.055004)

PACS numbers: 52.59.Ye, 42.65.-k, 52.25.Os, 52.38.-r

The terahertz (THz) generation methods based on the use of laser-induced plasmas are of great interest at present. These methods are usually realized under the ionization of different gases, including ambient air, by femtosecond laser pulses. The great interest in these methods is due to the capabilities of obtaining coherent, intense, broadband, and highly directional THz pulses (see, e.g., a review in [1]). In addition, the laser-plasma generation techniques can be coupled with the laser-plasma detection techniques which also have a superior bandwidth and are realized under the ambient air ionization [1,2]. Because of these capabilities, there are fine prospects of using laser-plasma schemes for THz spectroscopy of different materials. There is an especially attractive possibility of remote location of the generating and detecting laser-induced plasma to avoid transport of the THz radiation strongly absorbed in the atmospheric air.

At present, the most popular and efficient laser-plasma schemes of THz generation are the so-called two-color schemes, in which the laser pulse at the fundamental frequency is supplemented by its second harmonic obtained using a nonlinear crystal. These schemes have provided THz pulses with electric fields of up to 1 MV/cm or higher [3–7]. The capabilities of THz polarization and spectrum control by varying the polarization, duration, and focusing of two-color pulses have been demonstrated [3,8–13]. The THz spectrum usually contains a low-frequency core in the range of a few THz (typically, 1–3 THz), where the main energy of the THz pulse is concentrated, and a long high-frequency tail, which can spread to tens of THz [3,7–9,14]. The latter can be attributed to the currents varying rapidly under the laser pulse action. The main contribution to the low-frequency THz radiation is made by the plasma currents in the long wakefield of the laser pulse. The amplitude of the low-frequency currents is determined by the

free-electron residual current density (RCD) [15–17], which is equal to the zero-frequency spectrum of the time derivative of the current density excited during ionization. In several papers, amplification of the high-frequency THz radiation has been studied when using *incommensurate* pulses, in which the frequency of the additional field is detuned and the frequency ratio in the two-color pulse is not exactly equal to 2 [4,14,18]. However, the important issue of how this detuning affects the more efficient low-frequency THz generation is still unexamined, both in experiment and in theory.

Our Letter is the first-ever attempt of implementing independent control of the additional-field frequency detuning as well as of the mutual polarization and the powers of the main and additional fields in order to focus on the study of low-frequency THz generation in two-color laser-plasma schemes. This independent control allows us to verify the analytical approach to RCD calculation that we develop. The approach is based on calculation of the ionization-induced electron-density harmonics at the frequencies of the main and additional fields. Using this approach, we obtain closed-form analytical formulas, which determine RCD dependences on all parameters of two-color pulses and can be easily compared with experimental results. The optical parametric amplifier (OPA) used in our experiment produces an additional field tunable near the half-harmonic frequency. It can be said that this scheme is inverted with respect to the common two-color scheme since the double-frequency field is the main strong field in our case. The use of lower-frequency pumping fields produced by OPA can increase the efficiency of THz generation, as it was shown in [7], where the OPA-generated frequency-tunable pulse and its second harmonic were utilized. Moreover, the dephasing length determined by the air dispersion [3,19] for two-color pulses with waves at 800

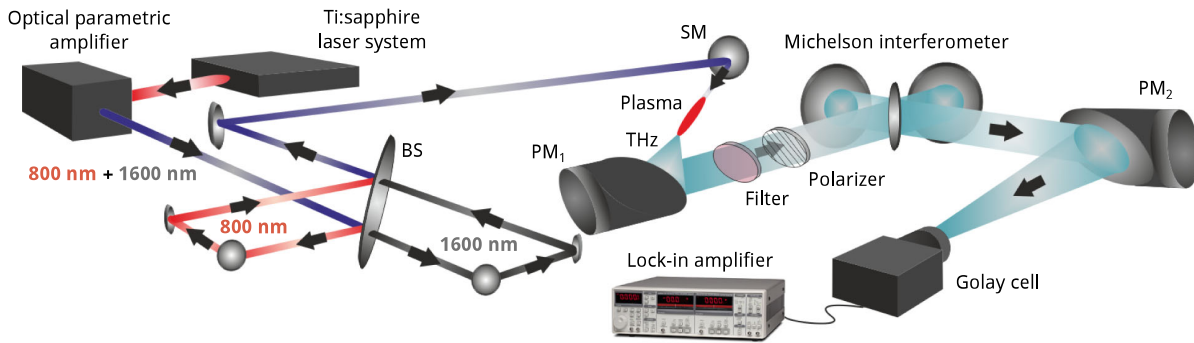


FIG. 1 (color online). Experimental setup. Femtosecond fundamental- and half-harmonic pulses from the OPA are separated by a spectral beam splitter (BS). After this, each pulse passes the delay line, where the polarization and energy in each pulse are controlled by polarization attenuators (not shown). The pulses are joined on BS, are focused using a spherical mirror (SM), and ionize the air, producing a plasma. THz radiation from the plasma is sent into a Michelson interferometer (in autocorrelation measurements) by a parabolic mirror ( $PM_1$ ) through a polarizer and a filter (teflon and black polyethylene) blocking the optical radiation and is focused on a Golay cell by another parabolic mirror ( $PM_2$ ).

and 1600 nm is 4 times greater than that for the pulses with waves at 800 and 400 nm (10 cm against 2.5 cm). This allows employing looser focusing of the laser pulse and longer plasma filament without destructive interference of the THz radiation [13,20], thus achieving a higher THz yield.

A schematic of our experiment is shown in Fig. 1. The OPA (TOPAS, Light Conversion Ltd.) was pumped by a Ti:sapphire laser system (Spitfire, Spectra Physics) delivering laser pulses with the duration of 50 fs, energy of 1.3 mJ, repetition rate of 1 kHz, and central wavelength of 800 nm. We employed the radiation at 800 nm with a pulse energy of up to 800  $\mu$ J that remained after the OPA and the OPA-generated idler wave tunable near the half-harmonic wavelength at 1600 nm with a pulse energy of up to 80  $\mu$ J. Both waves were linearly polarized in the horizontal plane. These waves were separated using a spectral beam splitter and were sent to the delay lines. The average power and polarization direction in each wave were controlled independently using polarization attenuators consisting of a half-wave plate and polarizer. After the delay lines, the two pulses were joined on the same beam splitter. The resulting 1-mm-diameter two-color beam was focused by a spherical mirror ( $f = 12.5$  cm), which corresponded to estimated spot sizes of 60 and 120  $\mu$ m for wavelengths of 800 and 1600 nm, respectively.

The forward THz emission from plasma string created in the focal region was collimated and was focused using two off-axis parabolic mirrors into a Golay cell. To measure separately the horizontal and vertical components of the THz yield, we used a wire grid polarizer. In some experiments, a Michelson interferometer containing a 10- $\mu$ m thick polyethyleneterephthalate film as a beam splitter was used for the autocorrelation measurements. To increase the signal-to-noise ratio, the optical radiation at 800 and 1600 nm was modulated by an optical chopper system with a two-frequency blade at frequencies 90 and 75 Hz,

respectively, and a signal from the Golay cell at the difference frequency of 15 Hz was measured with a lock-in amplifier (SRS830, Stanford Research). Since the OPA-generated idler wave used parametric fluorescence as a seed, the phase shift of the idler wave relative to the pump wave was random and varied from pulse to pulse. Thus, the signal from a Golay cell provided an averaged (over phase shift) THz yield.

In our experiments, we observed a number of effects which are very important both for the THz yield control and for the development of the theoretical model (see Fig. 2). First, this concerns the dependences [shown in Fig. 2(a)] of the horizontal and vertical components of the THz yield on the angle  $\theta$  between the fundamental-harmonic field (oriented horizontally) and the half-harmonic field. For small  $\theta$ , the THz polarization is mainly horizontal and the THz yield is maximal. As  $\theta$  increases, the horizontal component of the THz field decays while the vertical one rises and reaches a maximum at  $\theta \approx \pi/4$ . For greater  $\theta$ , both components fall, and at  $\theta = \pi/2$  the THz radiation disappears almost completely. Second, we measured the THz yield with independent variations in average powers of the fundamental- and half-harmonic fields. We found that, while the dependence of the THz yield on the half-harmonic power is simply quadratic, the dependence on the fundamental-harmonic power demonstrates very strong (exponential) threshold rise, as is shown in Fig. 2(b). Finally, we observed that, when *incommensurate* two-color pulses are used, the dependence of the THz yield on the half-harmonic detuning frequency has the resonant-like shape with the maximum near the zero detuning and a half-width of about 5 THz, as is shown in Fig. 2(c). At the same time, the low-frequency THz spectrum recovered (with regard to the spectral response of the detection system) from the autocorrelation measurements shown in Fig. 2(d) does not depend on the detuning and has both

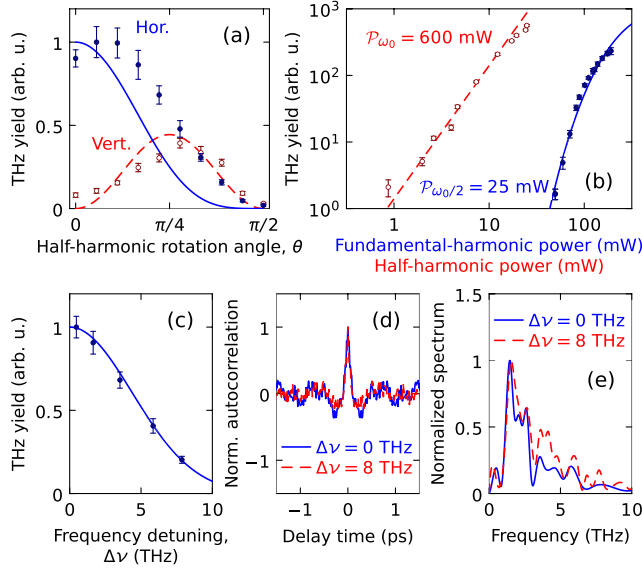


FIG. 2 (color online). (a)–(c) The THz yield as a function of the parameters of a two-color femtosecond pulse containing fundamental- and half-harmonic fields (the points are the experimental results, and the lines are obtained using analytical formulas; error bars correspond to the maximum and minimum values in a series of measurements). (a) Dependences of the horizontal (filled dots and solid line) and vertical (hollow dots and dashed line) polarization of the THz radiation on the half-harmonic rotation angle  $\theta$  (the angle between the fundamental- and half-harmonic fields) for the average powers of the fundamental harmonic  $\mathcal{P}_{\omega_0} = 600$  mW and the half harmonic  $\mathcal{P}_{\omega_0/2} = 30$  mW. (b) Dependence of the THz yield on  $\mathcal{P}_{\omega_0/2}$  for fixed  $\mathcal{P}_{\omega_0} = 600$  mW (hollow dots and dashed line) and dependence of the THz yield on  $\mathcal{P}_{\omega_0}$  for fixed  $\mathcal{P}_{\omega_0/2} = 25$  mW (filled dots and solid line). (c) Dependence of the THz yield obtained using *incommensurate* two-color pulses on the additional-field frequency detuning  $\Delta\nu$  (determined with an accuracy better than 50 GHz) with respect to the half-harmonic frequency for  $\mathcal{P}_{\omega_0} = 500$  mW and  $\mathcal{P}_{\omega_0/2} = 25$  mW. (d), (e) The normalized autocorrelation functions (d) and the corresponding normalized THz spectra (e) measured experimentally with (dashed line) and without (solid line) frequency detuning for  $\mathcal{P}_{\omega_0} = 500$  mW and  $\mathcal{P}_{\omega_0/2} = 25$  mW.

the central frequency  $f_{\text{THz}}$  and the width at the half-peak level of about 1.5 THz [see Fig. 2(e)].

To explain the results of the experiment, we use a theoretical model based on the following concept. Since  $f_{\text{THz}} \ll 1/\tau_p$  at the laser pulse duration  $\tau_p \lesssim 100$  fs, the optical-to-THz conversion process can be divided into two stages having significantly different time scales [15,21,22]. At the first short stage the electric field of a femtosecond laser pulse ionizes the air and accelerates the newly freed electrons, imparting to them, besides the oscillatory velocity, a dc drift velocity. With certain phase relations between the main and additional fields, the drift velocities of electrons are predominantly unidirectional [3], which may lead to the occurrence of a significant RCD by the end of the first stage. The RCD is an initial

impetus to the excitation of self-consistent fields and currents in the plasma produced [15,21]. At a long second stage of the process, which has a picosecond time scale  $\sim 1/f_{\text{THz}}$ , these currents relax in the plasma and radiate electromagnetic waves. The relaxation time is mainly determined by a characteristic plasma frequency, electron collision frequency, and plasma string diameter [15,21,22], all of which correspond to the THz band under conditions of our experiment, as well as in most experiments on air ionization by femtosecond laser pulses [8,14,20,21].

When we interpret the results of our experiments, we focus only on the first stage of the optical-to-THz conversion, i.e., on RCD calculation, since the THz yield is proportional to RCD squared. The local current density  $\mathbf{j}$  at the first stage depends on the time  $t$  and varies under the action of a laser electric field  $\mathbf{E}(t)$ . To calculate  $\mathbf{j}(t)$  and the free-electron density  $N(t)$ , we use the *semiclassical* approach, which consists of the solution of the following equations [7,13–16]:

$$\frac{\partial \mathbf{j}}{\partial t} + \nu \mathbf{j} = \frac{e^2}{m} N \mathbf{E}, \quad \frac{\partial N}{\partial t} = (N_g - N)w(E). \quad (1)$$

Here,  $N_g$  is the undisturbed gas density,  $\nu$  is the electron collision frequency,  $e$  and  $m$  are the electron charge and mass, respectively, and  $w(E)$  is the tunneling ionization probability per unit time.

Under the assumption that  $N \ll N_g$  and  $\nu\tau_p \ll 1$ , the RCD  $\mathbf{j}_{\text{RCD}}$  is a solution of Eqs. (1) for  $\nu = 0$  and  $t \rightarrow \infty$ ,

$$\mathbf{j}_{\text{RCD}} = \frac{e^2}{m} \int_{-\infty}^{\infty} N \mathbf{E} dt, \quad N(t) = N_g \int_{-\infty}^t w dt. \quad (2)$$

We use Eqs. (2) to find approximate analytical formulas for RCD by using a new approach based on calculation of the harmonics of  $N$  at the frequencies of the main and additional fields while allowing for the finiteness of the laser pulse duration. In our analytical calculations,  $\mathbf{E}(t)$  is specified as follows:

$$\begin{aligned} \mathbf{E}(t) = & \mathbf{E}_{\omega_0}(t) \cos \omega_0 t \\ & + \mathbf{E}_{\omega_0/2}(t) \cos [(\omega_0/2 - \Delta\omega)t + \phi]. \end{aligned}$$

Here,  $\omega_0$  is the fundamental (carrier) frequency,  $\Delta\omega \ll \omega_0/2$  is the small detuning of the half-harmonic frequency,  $\phi$  is the phase shift between the carriers of additional and main fields, and  $\mathbf{E}_{\omega_0}(t) = E_{\omega_0}(t)\hat{\mathbf{x}}$  and  $\mathbf{E}_{\omega_0/2}(t) = E_{\omega_0/2}(t)(\cos \theta \hat{\mathbf{x}} + \sin \theta \hat{\mathbf{y}})$  are the slowly time-dependent amplitudes of the fundamental- and half-harmonic fields, respectively.

Assuming that the characteristic time of ionization  $\tau_i$  is much greater than the half-harmonic period  $T = 4\pi/\omega_0$ , we can represent the RCD as

$$\mathbf{j}_{\text{RCD}} \approx \frac{e^2}{m} \int_{-\infty}^{\infty} \overline{N\mathbf{E}} dt, \quad (3)$$

where the slowly time-dependent period-averaged product of  $N$  and  $\mathbf{E}$  is

$$\overline{N\mathbf{E}} = \frac{1}{2} \text{Re} [\mathbf{E}_{\omega_0/2}(t) N_{\omega_0/2}(t) e^{-i\phi+i\Delta\omega t} + \mathbf{E}_{\omega_0}(t) N_{\omega_0}(t)].$$

Here,  $N_{\omega_0}(t)$  and  $N_{\omega_0/2}(t)$  are the complex amplitudes (slow envelopes) of the density oscillations at the fundamental and half-harmonic frequencies, respectively,

$$N_{\Omega}(t) = \frac{2}{T} \int_{t-T/2}^{t+T/2} N e^{-i\Omega t} dt \approx -\frac{2iN_g}{T\Omega} \int_{t-T/2}^{t+T/2} w e^{-i\Omega t} dt, \quad (4)$$

where  $\Omega$  takes the values  $\omega_0/2$  and  $\omega_0$ . We assume that  $E_{\omega_0/2} \ll E_{\omega_0}$  and  $w(E)$  is a sharp function, i.e.,  $Ew'(E)/w(E) \gg 1$ , where the prime denotes a derivative with respect to the argument. In this case, the function  $w[E(t)]$  has four sharp maxima on the time interval  $T$ , which are located near the maxima of  $|\cos \omega_0 t|$ . This allows one to use Laplace's method for calculation of integral (4) and find that

$$N_{\omega_0/2}(t) \approx -\frac{2iN_g \cos \theta}{\omega_0} \bar{w}'(E_{\omega_0}) E_{\omega_0/2} e^{-i\phi+i\Delta\omega t}, \quad (5)$$

$$\text{Re } N_{\omega_0}(t) \approx -\frac{N_g \cos^2 \theta}{2\omega_0} \frac{\bar{w}'(E_{\omega_0}) E_{\omega_0/2}^2}{E_{\omega_0}} \sin(2\Delta\omega t - 2\phi), \quad (6)$$

$$\overline{N\mathbf{E}} \asymp (N_g/4\omega_0) \bar{w}'(E_{\omega_0}) E_{\omega_0/2}^2 \times \sin(2\Delta\omega t - 2\phi) (3 \cos^2 \theta \hat{\mathbf{x}} + 2 \sin 2\theta \hat{\mathbf{y}}), \quad (7)$$

where  $\bar{w}(E_{\omega_0}) = [2w^3(E_{\omega_0})/\pi E_{\omega_0} w'(E_{\omega_0})]^{1/2}$  is the average ionization rate for sharp function  $w(E_{\omega_0})$  and  $\bar{w}' \approx \bar{w}w'/w$ . Taking into account that  $\bar{w}(E_{\omega_0})$  is a sharp function of  $t$  near its maximum with time width of  $\tau_i$ , we can write that  $\bar{w}[E_{\omega_0}(t)] \approx \bar{w}(E_1) \exp(-t^2/2\tau_i^2)$ , where  $E_1$  is the maximum fundamental-harmonic amplitude and  $\tau_i = [d^2 E_{\omega_0}/dt^2|_{t=0} \bar{w}'(E_1)/\bar{w}(E_1)]^{-1/2}$ . Considering that  $\tau_i$  is much less than the laser pulse duration, and substituting Eq. (7) into Eq. (3), we find that

$$\mathbf{j}_{\text{RCD}} \approx \frac{\sqrt{2\pi}}{4} j_{\text{osc}} \frac{\bar{w}'(E_1)}{E_1} \tau_i e^{-2(\tau_i \Delta\omega)^2} E_{1/2}^2 \Phi(\phi, \theta), \quad (8)$$

$$\Phi(\phi, \theta) = -\sin 2\phi [3 \cos^2 \theta \hat{\mathbf{x}} + 2 \sin 2\theta \hat{\mathbf{y}}], \quad (9)$$

where  $j_{\text{osc}} = e^2 N_g E_1 / m \omega_0$  is the maximum oscillatory current density in the main field and  $E_{1/2}$  is the maximum half-harmonic amplitude.

According to analytical formulas (8) and (9), the RCD depends on the half-harmonic power  $\mathcal{P}_{\omega_0/2} \propto E_{1/2}^2$ , the angle  $\theta$ , and the phase shift  $\phi$  (over which the averaging is performed for RCD squared when comparing with the experiment) as the product of separate functions, each being independent of a specific form of the function  $w(E)$ . This allows one to explain very clearly the experimental results. First, this concerns the dependences of the horizontal and vertical components of the THz yield  $\mathcal{P}_{\text{hor}} \propto j_{\text{RCD}_x}^2 \propto 9 \cos^4 \theta$  and  $\mathcal{P}_{\text{vert}} \propto j_{\text{RCD}_y}^2 \propto 4 \sin^2 2\theta$  on the angle  $\theta$  [see Fig. 2(a)]. Strong suppression of the THz radiation at  $\theta = \pi/2$  can be explained by the disappearance of the density harmonics  $N_{\omega_0/2}$  and  $N_{\omega_0}$  for  $E_{\omega_0/2} \ll E_{\omega_0}$ , since they are proportional to the dot product  $\mathbf{E}_{\omega_0/2} \mathbf{E}_{\omega_0}$  and its square, respectively, due to the Taylor approximation of  $w[E(t)]$  when integral (4) is calculated. Some maxima shift in the experimental data can be explained by an uncertain alignment of the THz polarizer with limited contrast ratio. Second, the formulas describe very well the dependence of the THz yield on the half-harmonic power for a fixed fundamental-harmonic power [see Fig. 2(b)]. In addition, these formulas describe the high sensitivity of the THz yield to a frequency detuning. With the detuning, the phase shift between the carriers of half- and fundamental-harmonic fields becomes time dependent. This leads to destructive superposition of the contributions to average drift velocity from the electrons born at different values of the phase shift. Equation (8) is exactly an indication that if this shift changes drastically over the ionization time  $\tau_i$ , the total RCD is significantly attenuated.

The experimentally observed very strong rise in the THz yield with increasing fundamental-harmonic power can be explained by a strong (exponential) dependence  $w(E)$  and, correspondingly, the similar dependence of the number of free electrons responsible for the THz generation. To compare the experiment with the theory, we substitute the well-known formula [4,12,14]  $w(E) = (\alpha \Omega_a E_a / E) \exp(-\beta E_a / E)$  in Eq. (8). Here,  $E_a = 5.14 \times 10^9$  V/cm and  $\Omega_a = 4.13 \times 10^{16}$  s<sup>-1</sup> are the atomic units of the field and frequency, respectively;  $\alpha = 4(I_{N_2}/I_H)^{5/2}$  and  $\beta = (2/3)(I_{N_2}/I_H)^{3/2}$ , where  $I_{N_2} = 15.6$  eV and  $I_H = 13.6$  eV are the ionization potentials of a nitrogen molecule and a hydrogen atom, respectively. Assuming that  $E_{\omega_0}(t) = E_1 \exp[-2(\ln 2)t^2/\tau_p^2]$ , where  $\tau_p$  is the intensity FWHM, we find that

$$\mathbf{j}_{\text{RCD}} \approx j_{\text{osc}} (\alpha \beta^{1/2} \Omega_a \tau_i / 2) (E_a / E_1)^{3/2} \times e^{-\beta E_a / E_1} e^{-2(\tau_i \Delta\omega)^2} (E_{1/2} / E_1)^2 \Phi(\phi, \theta), \quad (10)$$

$$\tau_i = \tau_p \sqrt{E_1 / 4(\ln 2) \beta E_a}. \quad (11)$$

The closed-form formulas (10) and (11) are in a very good agreement with the experimentally measured dependences of the THz yield on the fundamental-harmonic power  $\mathcal{P}_{\omega_0} \propto E_1^2$  [see Fig. 2(b)] and the frequency detuning  $\Delta\nu = \Delta\omega/2\pi$  [see Fig. 2(c)]. The dependence on  $\Delta\nu$  has the form of a resonantlike curve with a FWHM of  $\sqrt{\ln 2}/2\pi\tau_i$ . Thus, for *incommensurate* two-color pulses, the key parameter that determines the efficiency of low-frequency THz generation is  $\tau_i\Delta\omega$ . As this parameter increases, the THz yield decreases exponentially. Here, one can see an analogy with the use of one-color few-cycle laser pulses [15–17,23], where the efficiency of low-frequency THz generation is determined by the value of the parameter  $\tau_i\omega_0$  in the same way.

To conclude, we have measured for the first time the parameters of the low-frequency THz radiation generated in the experiment with the ambient air ionized by a two-color femtosecond pulse containing the field at the fundamental frequency of a Ti:sapphire laser and an OPA-generated additional field tunable near the half-harmonic frequency. By realizing independent control of the additional-field frequency detuning as well as of the mutual polarization and the powers of the main and additional fields, we have observed several effects that are described very well by the features of the RCD excitation in a laser-induced plasma. The most important new effect, which has been demonstrated, is resonantlike sensitivity of the low-frequency THz yield to the additional-field frequency detuning. To interpret experimental dependences of the THz power and polarization on the parameters of the two-color pulse, we have obtained closed-form analytical formulas by using the new approach to RCD determination. This approach is based on calculations of free-electron density harmonics at the frequencies of the main and additional fields with allowance for the finiteness of the laser duration. This approach can be easily extended to calculate the ionization-induced currents in a wide range of ultrafast strong-field phenomena based on generation of harmonics and combination frequencies, which can be both less and greater than laser frequencies.

This work was supported by the Government of the Russian Federation (Agreement No. 14.B25.31.0008), the Ministry of Education and Science of the Russian Federation (Agreement No. 14.B37.21.0770), and the Russian Foundation for Basic Research (Grants No. 11-02-01416, No. 12-02-31424, No. 12-01-31270, No. 12-02-33087, No. 12-02-12101, and No. 13-02-00964).

---

\*vved@appl.sci-nnov.ru

- [1] B. Clough, J. Dai, and X.-C. Zhang, *Mater. Today* **15**, 50 (2012).  
 [2] J. Liu, J. Dai, S. L. Chin, and X.-C. Zhang, *Nat. Photonics* **4**, 627 (2010); Z. Lü, D. Zhang, C. Meng, L. Sun, Z. Zhou, Z. Zhao, and J. Yuan, *Appl. Phys. Lett.* **101**, 081119 (2012).

- [3] K. Y. Kim, J. H. Glowonia, A. J. Taylor, and G. Rodriguez, *Opt. Express* **15**, 4577 (2007); K. Y. Kim, A. J. Taylor, J. H. Glowonia, and G. Rodriguez, *Nat. Photonics* **2**, 605 (2008).  
 [4] M. D. Thomson, V. Blank, and H. G. Roskos, *Opt. Express* **18**, 23173 (2010).  
 [5] T. I. Oh, Y. S. You, N. Jhajj, E. W. Rosenthal, H. M. Milchberg, and K. Y. Kim, *New J. Phys.* **15**, 075002 (2013).  
 [6] Y. Minami, T. Kurihara, K. Yamaguchi, M. Nakajima, and T. Suemoto, *Appl. Phys. Lett.* **102**, 041105 (2013).  
 [7] M. Clerici, M. Peccianti, B. E. Schmidt, L. Caspani, M. Shalaby, M. Giguère, A. Lotti, A. Couairon, F. Légaré, T. Ozaki, D. Faccio, and R. Morandotti, *Phys. Rev. Lett.* **110**, 253901 (2013).  
 [8] A. V. Borodin, N. A. Panov, O. G. Kosareva, V. A. Andreeva, M. N. Esaulkov, V. A. Makarov, A. P. Shkurinov, S. L. Chin, and X.-C. Zhang, *Opt. Lett.* **38**, 1906 (2013).  
 [9] J. M. Manceau, A. Averchi, F. Bonaretti, D. Faccio, P. Di Trapani, A. Couairon, and S. Tzortzakis, *Opt. Lett.* **34**, 2165 (2009).  
 [10] D. Dietze, J. Darmo, S. Roither, A. Pugzlys, J. N. Heyman, and K. Unterrainer, *J. Opt. Soc. Am. B* **26**, 2016 (2009).  
 [11] J. Dai, N. Karpowicz, and X.-C. Zhang, *Phys. Rev. Lett.* **103**, 023001 (2009).  
 [12] H. Wen and A. M. Lindenberg, *Phys. Rev. Lett.* **103**, 023902 (2009).  
 [13] G. Rodriguez and G. L. Dakovski, *Opt. Express* **18**, 15130 (2010).  
 [14] I. Babushkin, S. Skupin, A. Husakou, C. Köhler, E. Cabrera-Granado, L. Bergé, and J. Herrmann, *New J. Phys.* **13**, 123029 (2011).  
 [15] V. B. Gildenburg and N. V. Vvedenskii, *Phys. Rev. Lett.* **98**, 245002 (2007); H.-C. Wu, J. Meyer-ter Vehn, and Z.-M. Sheng, *New J. Phys.* **10**, 043001 (2008); C. S. Liu and V. K. Tripathi, *J. Appl. Phys.* **105**, 013313 (2009).  
 [16] A. A. Silaev and N. V. Vvedenskii, *Phys. Rev. Lett.* **102**, 115005 (2009); A. A. Silaev and N. V. Vvedenskii, *Phys. Scr.* **T135**, 014024 (2009).  
 [17] A. A. Silaev, M. Y. Ryabikin, and N. V. Vvedenskii, *Phys. Rev. A* **82**, 033416 (2010); L. N. Alexandrov, M. Y. Emelin, and M. Y. Ryabikin, *ibid.* **87**, 013414 (2013).  
 [18] F. Théberge, M. Châteauneuf, G. Roy, P. Mathieu, and J. Dubois, *Phys. Rev. A* **81**, 033821 (2010); T. Balčiūnas *et al.*, in *International Conference on Ultrafast Phenomena (Optical Society of America, 2010)* p. PDP4.  
 [19] P. E. Ciddor, *Appl. Opt.* **35**, 1566 (1996).  
 [20] Y. Liu, A. Houard, M. Durand, B. Prade, and A. Mysyrowicz, *Opt. Express* **17**, 11480 (2009); Y. S. You, T. I. Oh, and K. Y. Kim, *Phys. Rev. Lett.* **109**, 183902 (2012); L. Bergé, S. Skupin, C. Köhler, I. Babushkin, and J. Herrmann, *ibid.* **110**, 073901 (2013).  
 [21] V. A. Kostin and N. V. Vvedenskii, *Opt. Lett.* **35**, 247 (2010).  
 [22] N. Karpowicz and X.-C. Zhang, *Phys. Rev. Lett.* **102**, 093001 (2009).  
 [23] M. Kieß, T. Löffler, M. Thomson, R. Dörner, H. Gimpel, K. Zrost, T. Ergler, R. Moshhammer, U. Morgner, J. Ullrich, and H. Roskos, *Nat. Phys.* **2**, 327 (2006); Y. Bai, L. Song, R. Xu, C. Li, P. Liu, Z. Zeng, Z. Zhang, H. Lu, R. Li, and Z. Xu, *Phys. Rev. Lett.* **108**, 255004 (2012).